SCREEN-PRINTED RIBBON GROWTH ON SUBSTRATE SOLAR CELLS EXCEEDING 12% EFFICIENCY

S. Seren[1], G. Hahn[1], F. Huster [1], R. Kopecek[1], A. Gutjahr[2], A. R. Burgers[2], A. Schönecker[2]
[1]University of Konstanz, Department of Physics, D-78457 Konstanz, Germany, email: sven.seren@uni-konstanz.de
[2]ECN - Solar Energy, P.O. Box 1, 1755 ZG Petten, Netherlands, email: schonecker@ecn.nl

ABSTRACT: Ribbon Growth on Substrate (RGS) solar cells have been processed at the University of Konstanz using an adapted industrial-type fire-through SiN process. Efficiencies above 12% have been reached on 5x5 cm^2 cells processed from boron doped RGS material and efficiencies of 11% from gallium doped RGS material. These are the highest efficiencies obtained on this promising and cost-effective material using an industrial-type cell process. An important factor for the increase in efficiency is the reduced oxygen concentration of almost an order of magnitude in the current RGS wafer material compared to former RGS material. Enhanced J_{sc}, V_{oc}, especially in case of the gallium doped RGS material, and L_{eff} values in the range of 100 μm as well as lifetimes above 4 μs demonstrate the potential of the new low oxygen RGS material. No additional bulk passivation steps have to be performed, a sufficient passivation is guaranteed solely by hydrogen originating from a hydrogen rich SiN_x antireflective coating allowing a totally industrial-type cell process. An applied surface texture results in a gain in J_{sc} of more than 1 mA/cm^2 enabling efficiencies close to 13% using material of current quality.
Keywords: Ribbon Silicon, Shunts, Hydrogen

1 INTRODUCTION

Screen-printed Ribbon Growth on Substrate (RGS [1]) solar cells (5x5 cm^2) achieved efficiencies up to 10.5% using RGS wafer material with a high oxygen content [2]. Up to now this comparably high oxygen content > 10^{18} cm^{-3} was the main limiting factor for cell efficiencies due to several oxygen related defects like oxygen precipitates as well as formation of New Donors during wafer production or following high temperature solar cell processing steps. A rebuilding of the RGS machine and several improvements in the wafer process such as reduced melting temperatures allowed for lower oxygen contents down to 4x10^{17} cm^{-3}. This is comparable to standard cast multicrystalline material.

In this paper the main focus points are strongly enhanced J_{sc}, L_{diff} and τ values of solar cells produced from B doped low [O_i] RGS wafers leading to a record efficiency of 12.3% for an untextured cell.

Another approach presented is Ga doped RGS material. Due to the specific RGS crystal growth conditions a non uniform bulk doping of the wafers results in a drift-field supporting minority charge carriers to diffuse to the pn-junction. Enhanced short circuit current densities are the consequence.

Further on, a carbon related shunting mechanism as the most limiting factor for higher fill factors is discussed.

RGS wafers are currently produced by a laboratory scale R&D machine at ECN and solar cells are processed at the University of Konstanz (UKN) according to an industrial type screen-printing process [3].

2 CORRELATION OF [O_i] AND J_{sc}

Due to the rapid cooling of the cast RGS wafers after crystallisation of the liquid silicon, the formation of oxygen precipitates is inhibited and the oxygen remains preferentially dissolved on interstitial sites in the Si lattice. The concentration of the interstitial oxygen [O_i] as well as the concentration of the substitutional carbon [C_s] in the RGS wafer is determined by FTIR measurements. Fig. 1 shows a clear correlation between lower [O_i] in the as-grown wafer and a higher J_{sc} of the processed solar cell. Furthermore, a lower oxygen concentration results not only in larger diffusion lengths as can be seen in Fig. 2 but as well in a faster hydrogenation [4]. With lowering the oxygen content in the RGS wafer material shunt resistances of the processed solar cells seem to be affected. Fits to the dark IV curves revealed sometimes low shunt resistances resulting in poor fill factors for the low oxygen material.

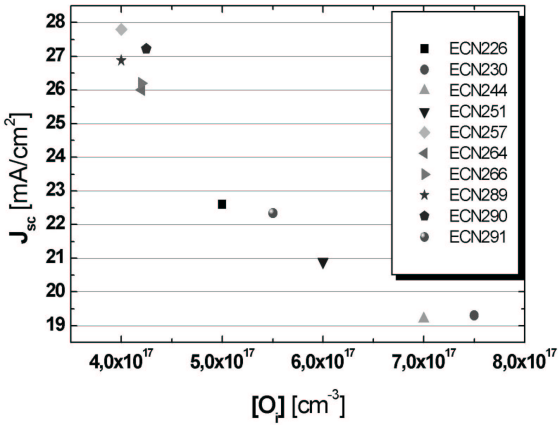

Figure 1: Dependence of J_{sc} on [O_i] for cells produced from various RGS production runs. Shown are average J_{sc} values of the respective solar cell runs.

screen printed RGS cell	V_{oc} [mV]	J_{sc} [mA/cm^2]	FF [%]	η [%]
high [O_i]				
4.9x4.9 cm^2	565	24.2	76.3	10.4
low [O_i]				
4.9x4.9 cm^2	580	28.1	75.6	12.3

Table 1: IV data of one of the best screen-printed RGS cells from low [O_i] RGS and high [O_i] RGS (older material) processed at UKN.

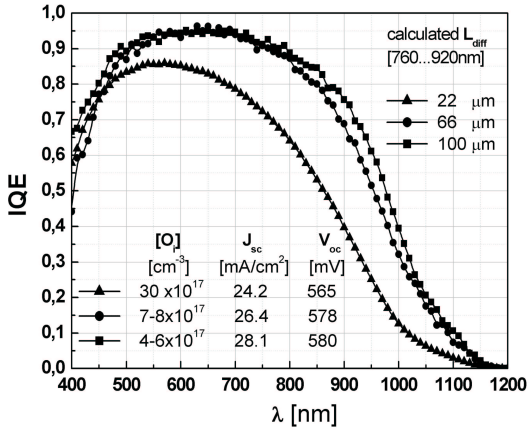

Figure 2: Increase of the diffusion length with lowered [O_i] for 3 representive cells produced from different RGS material.

The best cell produced from low [O_i] RGS material (run ECN 287) achieved a record efficiency of 12.3%. This result was confirmed by a measurement at an ISO 17025 accredited calibration laboratory, namely the European Solar Test Installation (ESTI) of the Joint Research Centre (JRC) of the European Commission. Compared to solar cells processed from high [O_i] RGS material, J_{sc} as well as V_{oc} could be enhanced resulting in higher efficiencies even though fill factors dropped most probably due to carbon related shunts in low [O_i] material. As soon as these material induced shunts can be avoided, efficiencies above 13% should easily be reached on untextured cells.

3 SURFACE TEXTURISATION

Different surface texturing methods were investigated to further increase J_{sc}. A wet chemical texture ($HNO_3/HF/H_2SO_4$) provided the best results on RGS material. An increase in J_{sc} of up to 1.1 mA/cm^2 could be reached on a textured cell compared to a cell without a surface texture originating from the same RGS wafer.

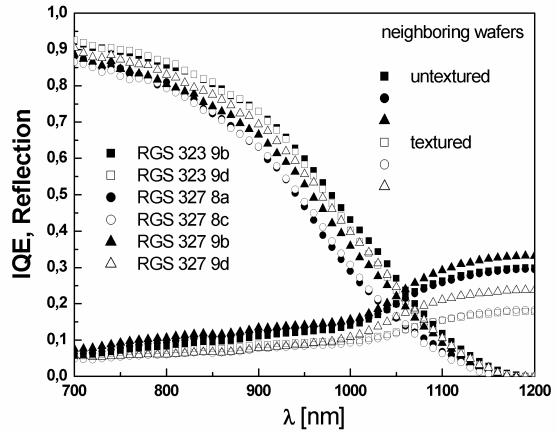

Figure 3: IQE and reflection data of solar cells originating from neighboring wafers (5x5 cm^2 cells originate from the same 12x8 cm^2 RGS wafer). Solid symbols indicate a flat cell surface, blank symbols an applied surface texture. The IQEs of the textured cells show a slight enhancement in the long wavelength range due to a better light trapping.

The RGS material is currently produced by a laboratory scale R&D machine with a limited amount of wafer output. Therefore texturisation experiments could not be performed on wafer material with highest lifetimes. Applying the texture to the material quality shown in Table 1 (12.3%), the increase in J_{sc} of 1.1 mA/cm^2 would result in an estimated efficiency of 12.9%.

4 BULK PASSIVATION

The RGS solar cell process as presented in [3] implies a microwave-induced remote hydrogen plasma (MIRHP) passivation step to passivate bulk defects followed by the deposition of a hydrogen-rich PECVD SiN_x layer, which acts as single layer antireflective coating. A comparison of the IV data of low [O_i] solar cells processed with and without a MIRHP passivation reveals that cell parameters only slightly increase by the MIRHP passivation..

screen-printed RGS cell	V_{oc} [mV]	J_{sc} [mA/cm^2]	FF [%]	η [%]
without additional MIRHP Passivation				
4.9x4.9 cm^2	582	28.1	73.4	11.98
with additional MIRHP Passivation				
4.9x4.9 cm^2	585	28.4	72.5	12.04

Table 2: IV data of solar cells processed from neighboring RGS wafers. The cell without the MIRHP passivation (RGS 276 6c) shows only a slightly lower efficiency compared to the MIRHP passivated cell (RGS 276 6a).

Due to the faster diffusion of hydrogen in low [O_i] RGS the hydrogen originating from the SiN_x antireflection coating is sufficiently distributed throughout the entire bulk of the solar cell during the short time period of contact firing. Thus the MIRHP bulk passivation can be omitted ending up with a totally industrial compatible solar cell process concerning bulk passivation.

5 DRIFT CELL

Besides B doped RGS material, Ga doped RGS wafers were produced. Ga as a dopant has the advantage to avoid recombination active boron-oxygen complexes degrading lifetimes. On the other hand Ga as a dopant in the RGS process results in a depth dependent dopant concentration in the wafers. This is a well known effect due to the low segregation coefficient for Ga in Si (k = 0.008) for low crystal growth velocities and has been applied e.g. to the EFG material in the past [5].

Opposite to almost steady state crystallisation, the RGS process is characterised by rapidly changing crystallisation speed with growing thickness of the wafer [6]. The initial high growth velocity results in k_{eff} close to unity at the beginning of wafer crystallisation. As crystal growth velocity decreases with increasing wafer

thickness, segregation becomes more effective. By controlling the thermal properties of the RGS wafer crystallisation, a gradient in dopant concentration throughout the wafer thickness can be achieved, enhancing the minority carrier transport towards the p-n junction by a drift field [7].

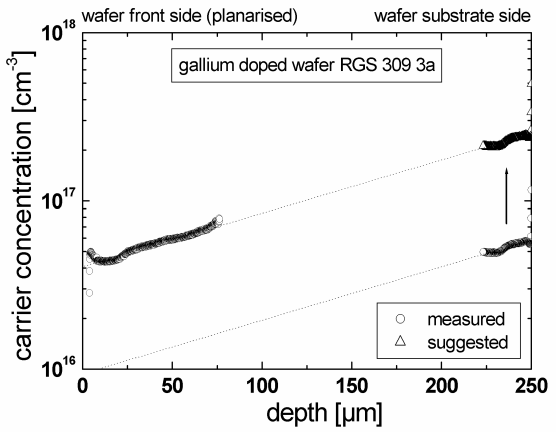

Figure 4: Bulk doping profile of a Ga doped RGS wafer. The doping concentration changes from $4x10^{16}$ cm^{-3} for the planarised wafer frontside to $2x10^{17}$ cm^{-3} for the wafer substrate side. It should be noted that the ECV measurement is afflicted with an inaccuracy of a factor of 2, due to surface roughness effects and side wall influences when etching into to the wafer. As front and back profiles origin from independent measurements, the overall profile is not necessarily following the line as indicated by the connection line.

As a result of the inhomogeneous bulk doping a drift field is formed. It is suggested that the field ranges through the entire wafer pointing from lower to higher doping concentrations (i.e from the wafer surface to the wafer substrate side). Minority charge carriers (electrons) would follow the drift field in opposite direction resulting in an enhanced J_{sc} of the processed solar cell. The simulated efficiency gain of a solar cell with typical RGS material parameters and a linear doping concentration gradient in the order of the measured values is 0.5% (abs.) due to the enhanced J_{sc} as compared to a solar cell with a uniform bulk doping concentration.

A pronounced gain in J_{sc} is observable for the wafers processed from the wafer front side (i.e. emitter formation on the wafer side with the lower doping concentration) due to the drift field. However, the absolute values of J_{sc} compared to the values of the cells processed from B doped RGS material are still lower. This could be explained by the higher overall bulk doping concentration of the Ga doped RGS material (0.3 Ωcm) compared to the B doped material (3 Ωcm) and better L_{eff} values of the latter. In addition the open circuit voltages obtained with the Ga doped material are much higher (> 15 mV) compared to the B doped material due to the higher bulk doping concentration near the emitter region (Table 3). It is expected that the results can be further improved by process optimization.

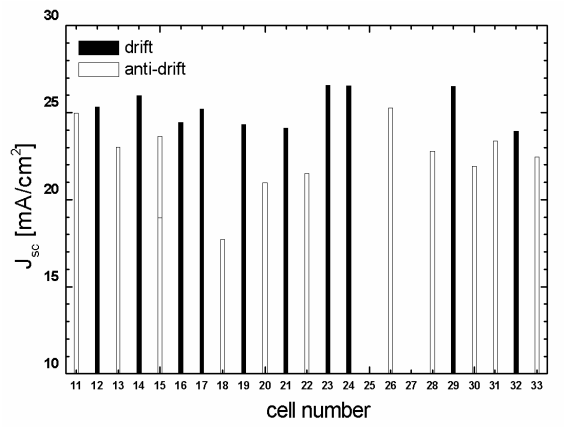

Figure 5: Comparison of J_{sc} values resulting from RGS wafers processed from the wafer front side (drift) and from the wafer substrate side (anti-drift).

screen-printed RGS cell	V_{oc} [mV]	J_{sc} [mA/cm^2]	FF [%]	η [%]
anti-drift cell				
4.9x4.9 cm^2	404	23.5	34.2	3.25
drift cell				
4.9x4.9 cm^2	596	26.3	68	10.7
best drift cell				
4.9x4.9 cm^2	603	26.6	68.6	11

Table 3: IV data of solar cells processed according to the drift and anti-drift concept from neighboring RGS wafers. Additionally, the IV data of the best Ga doped RGS cell is presented.

6 SHUNTING IN LOW [O_i] RGS

To investigate the sometimes poor shunt resistances in low [O_i] RGS wafer material, Lock-In Thermography measurements (VomoLIT or DLIT [8]) were performed on the processed solar cells. Fig. 6 shows widespread shunted regions (light areas) under forward and reverse bias. As a result nearly all shunts show an ohmic-type character (except one, marked with a circle).

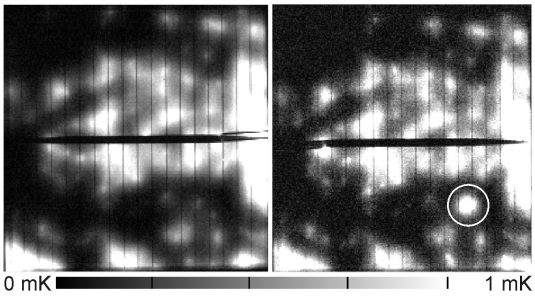

Figure 6: DLIT measurements in forward (+0.5 V, left) and reverse (-0.5 V, right) bias of the same solar cell originating from low [O_i] RGS material (run ECN 257). The same widespread shunted regions are visible in the reverse biased measurement.

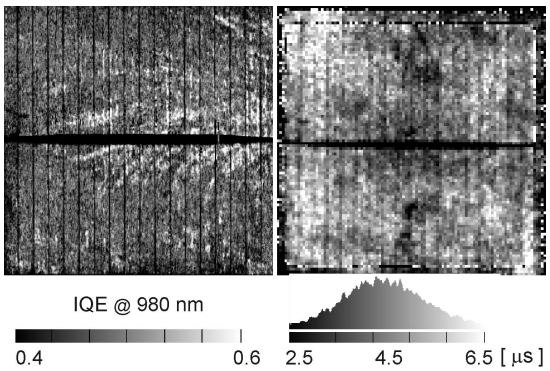

Figure 7: Left: IQE at 980 nm (same cell as in Fig. 6). The shunted regions in Fig. 6 are correlated to regions of enhanced IQE. Right: τ mapping of the same solar cell after removing of contacts, back surface field and emitter. The shunted regions can be related to areas with lower τ.

Average lifetimes > 4 µs were measured in shuntless regions of low [O_i] RGS. In contrast to that, shunted regions show a lowered τ (Fig. 7, right) but sometimes an enhanced IQE (Fig. 7, left). Therefore the enhanced IQE in these regions is not correlated to a larger L_{diff}. In these areas shunts are related to a current collecting mechanism, which draws off charge carriers generated next to the shunted regions. This kind of mechanism was already observed in high [O_i] RGS material. It was stated that due to oxygen precipitates current collecting inversion channels were formed [9,10]. As [O_i] is reduced in the current material, the effect shown in Fig. 7 might be related to SiC precipitates. The RGS material contains a high concentration of substitutional carbon in the range of $[C_s] = 1.2\text{-}1.8 \times 10^{18}$ cm^{-3}. This supersaturation and the presence of [O_i] enhances the formation of carbon precipitates especially at the bottom and the top of the wafer. In these wafer regions emitter and back surface field are formed during the following cell process steps. Carbon precipitates (like SiC) located in the space charge region of the emitter can form a conductive path between emitter and base. The widespread shunted regions shown in Fig. 6 are assumed to be caused by reticulated carbon precipitates propagating through the entire wafer as SiC related defects typically produce ohmic-type shunts [11]. However, further detailed investigations of the shunting mechanism are needed as also shunt-free RGS solar cells show identical [C_s] concentrations.

7 OUTLOOK

To reduce shunting in low [O_i] RGS wafer material, the carbon concentration should be reduced. It is expected that this will result in better fill factors and therefore in higher efficiencies.

Ga doped RGS material is a very promising approach due to the measured non uniform doping concentration and the resulting drift field enabling enhanced J_{sc} values. An optimisation of the concept, concerning the overall doping concentration and the distribution can lead to efficiencies above 13% with current material quality.

The surface of RGS material can be textured by acidic chemical etching. As this process becomes more standard in modern solar cell lines, it will also be applied to RGS wafers. On standard B doped wafers efficiencies around 13% are expected with today's material quality.

New substrate plates enabled the production of 10x10 cm^2 RGS wafers with a very small surface unevenness. According to this the planarisation step prior to cell processing could be omitted as well.

The production of n-type RGS material is in preparation. The advantages of n-type material are most likely transferable on RGS.

8 SUMMARY

Solar cells processed from RGS wafer material with reduced oxygen content show increased J_{sc} values using an industrial-type screen-printing fire through SiN process. Efficiencies up to 12.3% could be reached despite of relatively low fill factors in the range of 75% on untextured wafers. C correlated shunted regions in the wafer material itself are possibly responsible for the lower FFs. Enhanced J_{sc} and V_{oc} values already demonstrate the potential of the low [O_i] RGS material with efficiencies well above 13%, provided a surface texture is applied and shunting mechanisms can be avoided.

Ga doped RGS generates due to the specific crystal growth conditions during the RGS process a drift-field supporting minority charge carrier transport to the pn-junction.

9 ACKNOWLEDGEMENTS

Part of this work was funded by the EC in the RGSells project (ENK6-CT-2001-00574). The RGS wafer manufacturing process development is carried out in the RGSolar project supported by the Dutch EET programme under EETK 03023.

10 REFERENCES

[1] H. Lange *et al*, J. Cryst. Growth, 104 (1990) 108
[2] G. Hahn *et al*, Proc. 3rd WCPEC, Osaka 2003, 1285
[3] S. Seren *et al*, Proc. 31th IEEE PVSC, Lake Buena Vista 2005, in press
[4] G. Hahn *et al*, Proc. 19th EC PVSEC, Paris 2004, 427
[5] R. O. Bell *et al*, 18th IEEE PVSC, Las Vegas 1985, 764
[6] A. Schönecker *et al*, 12th NREL workshop on silicon solar cell materials, Breckenridge 2002, 7
[7] Patent pending.
[8] M. Kaes *et al*, Proc. 19th EC PVSEC, Paris 2004, 484
[9] O.Breitenstein *et al*, Solid State Phenomena 78-79 (2001) 29
[10] G. Hahn *et al*, Sol. Energy Mat. 72 (2002) 453-464
[11] H. Gottschalk *et al*, phys. stat. sol. (b) v.222, p. 353 (2000)